Temperature Fluctuations of the IGM and the Epoch of Reionization

Saleem Zaroubi
MPA

Collaborators:
T. Theuns
P. Tzanavaris, R.F. Carswell (IoA)
T.–S. Kim (ESO)
J. Schaye (IAS)

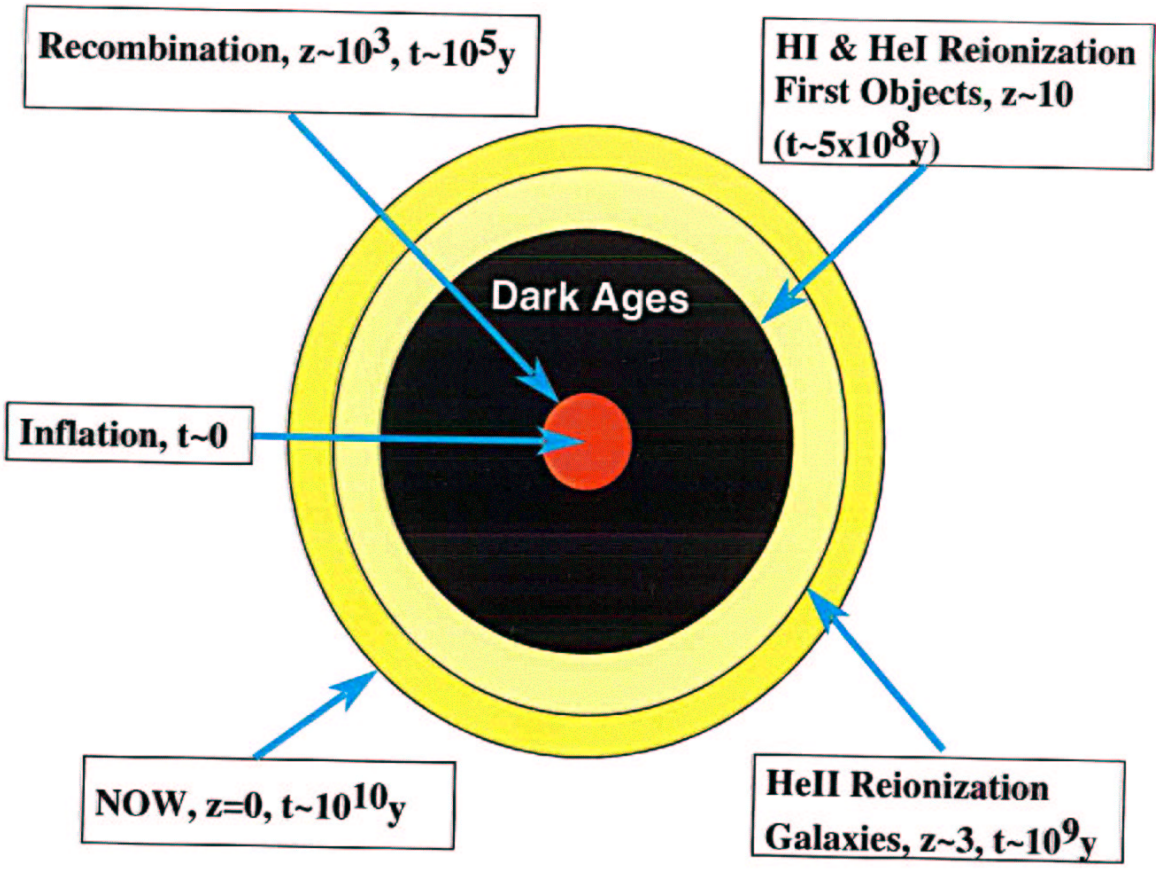

The Lyman–α Forest (Bahcall & Salpeter)

Absorption Features Blueward of the Ly–α emission line in quasar spectra.

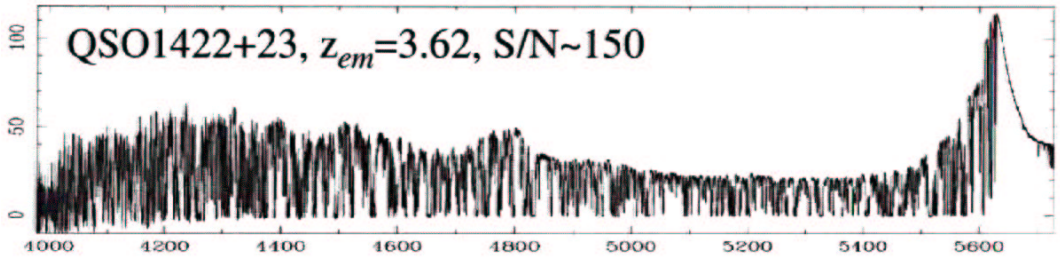

1– High Signal to Noise observations with 8m class telescopes at redshift range z~2–4.

2– High resolution hydrodynamic simulations of structure formation in cold–dark–matter universe (e.g., Cen *et al.* 94, ..., Theuns *et al.* 98)

Fluctuating Gunn–Peterson Effect

Normalized flux $F/F_c = e^{-\tau}$

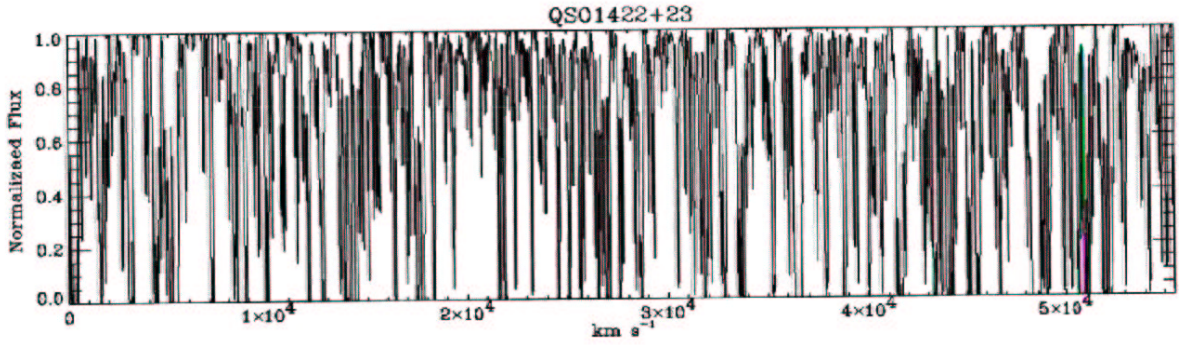

The optical depth, τ, for absorption of light that passes through the local Ly–α resonance is:

$$\tau(\lambda_{obs}) = \int_{z_{reion}}^{z_s} dz \frac{c\,dt}{dz} n_{HI}(z)\,\sigma_\alpha[\nu_{obs}(1+z)]$$

dl — HI number density — Scattering cross–section through Ly–α resonance

● The balance between the adiabatic cooling (due to expansion) and the UV background photo–heating introduce a tight relation between the temperature and density, (Hui & Gnedin 97)

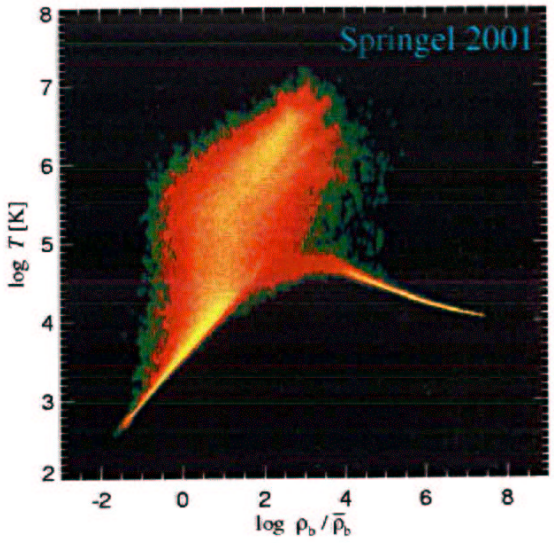

$$T = T_0 \left(\frac{\rho}{\langle \rho \rangle} \right)^{\gamma - 1}$$

Temp. of the IGM

(Efstathiou et al. 2000

● The Lyman–α forest is mainly produced by gas with:

$$\frac{\delta \rho}{\langle \rho \rangle} \leq 10$$

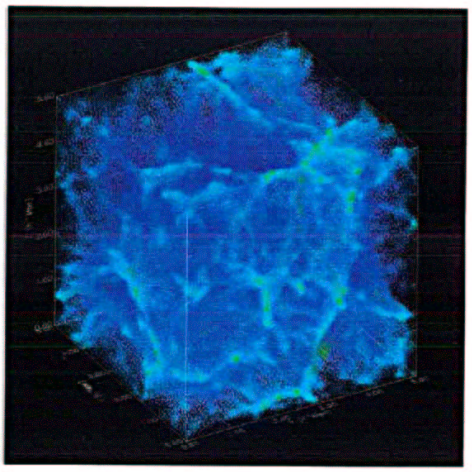

Z=3

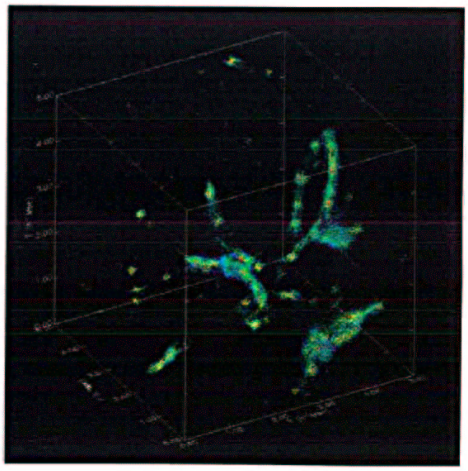

$T<10^5 K$

$T>10^5 K$

The Ly–α could therefore be used to learn about the properties of the diffuse IGM. In particular:

1. Optical depth of HI and HeII sets constraints on the baryonic density of the universe and on the evolution, amplitude and spectrum of the photo–ionizing background

2. On large scales, $R >> R_J$, the gas follows the dark matter and the Ly–α can be used to infer the matter overdensity at z~2–4 (Croft et al. 97, Nusser & Haehnelt 98).

3. On small scales, $R \sim R_J$, the pressure gradients are important. Hence, absorption linewidths can be used to infer the temperature and equation of state of the IGM. (Schaye *et al.* 2000, Theuns *et al.* 2000)

Previous Results – 1

1– Schaye *et al.* 2000 based on Voigt profile fitting deduced that there is a temperature jump at z~3.2

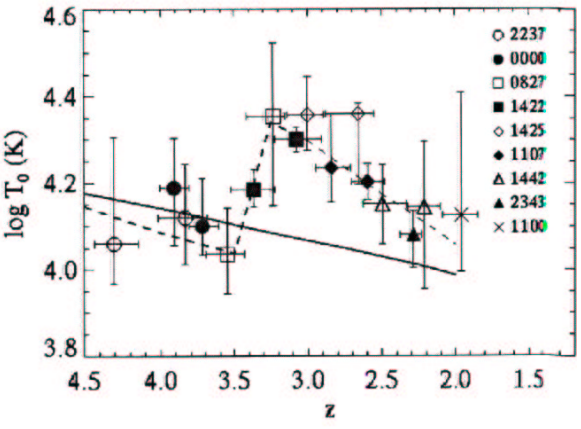

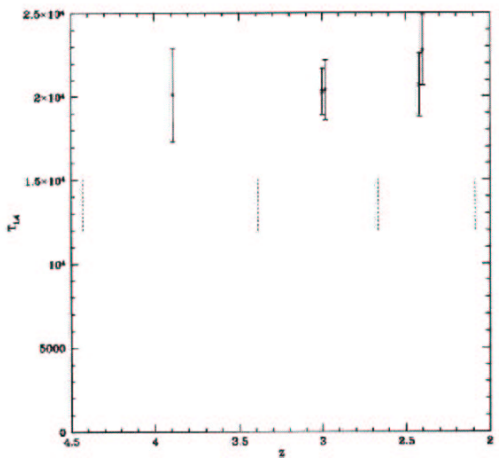

2– McDonald *et al.* 2000 deduced that there is NO temperature jump at z~3.2. Their analysis neglect Temp. dependence of Jeans smoothing

Previous Results – 2

3– Ricotti *et al.* 2000 used pseudo–hydrodynamical simulations and detected Temp. jump at 0.5 σ level

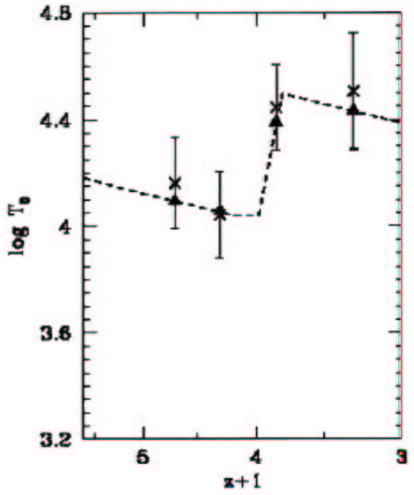

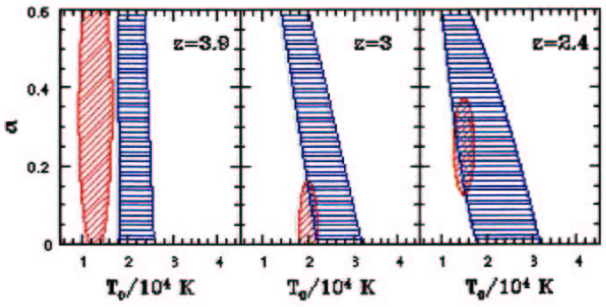

4– Zaladarriaga *et al.* 2001 deduced that there is NO temperature jump. Neglect Hydrodynamical effects in their analysis.

The Method

Spectrum is characterized with discrete wavelet transforms, and showed that:

1– PDF of wavelet amplitudes can be used to measure (T_0 & γ).

2– The positional information retained in the wavelet expansion coefficients allows detecting spatial variations in T_0 & γ

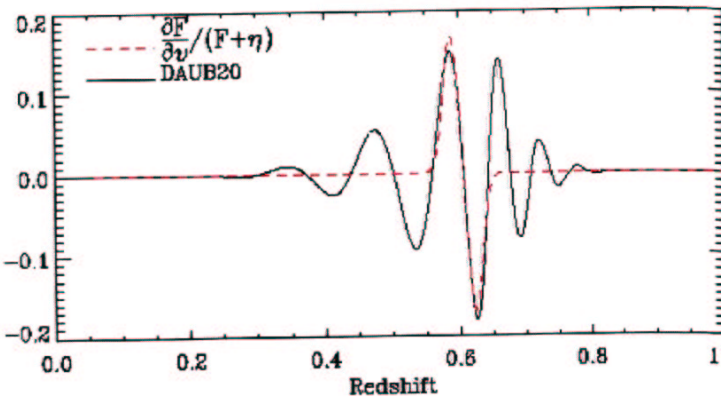

(Similar approachs were developed by Pando & Fang 96,98, Meiksin 00 & Zaldarriaga 01)

Simulations

(Theuns et al. 2001)

- SPH simulations based on the HYDRA code with Standard ΛCDM Universe.
- The simulated Box size of 7.7 Mpc comoving with 128^3 particles of each species
- The IGM is photo–ionized and –heated by the QSO induced UV background (Haardt & Madau 1996)

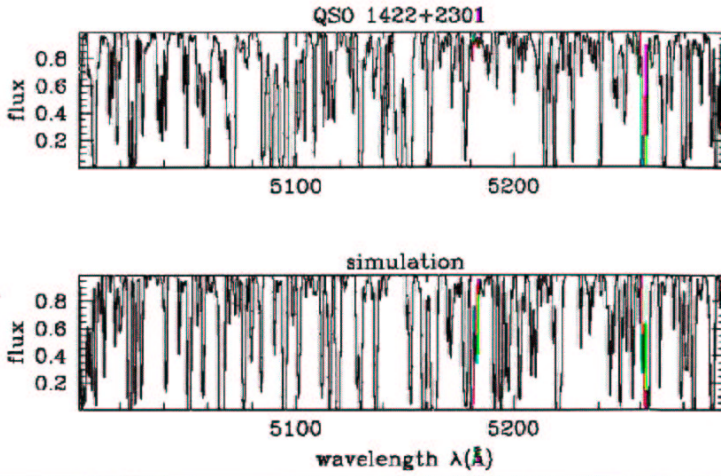

Three mock spectra are used to test the method, each with a specific equation of state & straddles a redshift range of V=50000 km/s

Spectrum	(T_0, γ)
S1	$(1.5\times10^{14},5/3)$ for $v \le V/2$ $(2.2\times10^{14},5/3)$ for $v \ge V/2$
S2	$(2.2\times10^{14},5/3)$ for $\lvert v - V/2\rvert > 2500$ $(1.5\times10^{14},5/3)$ else
S3	$(2.2\times10^{14},5/3)$

Wavelet expansion

Cold

Hot

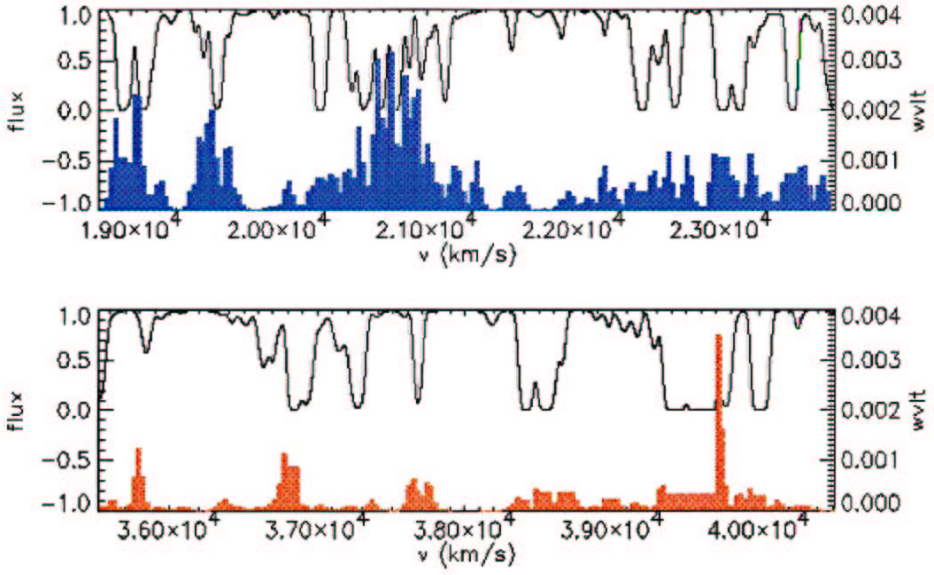

Flux (left) & wavelet amplitude (right) from 5000 km/s cold (upper panel) and hot (lower panel) stretches of spectra

Statistical analysis

Cumulative distribution of the wavelet Amplitude of S1 for the hot half, cold half and all spectrum. Vertical lines indicate maximum distances between them.

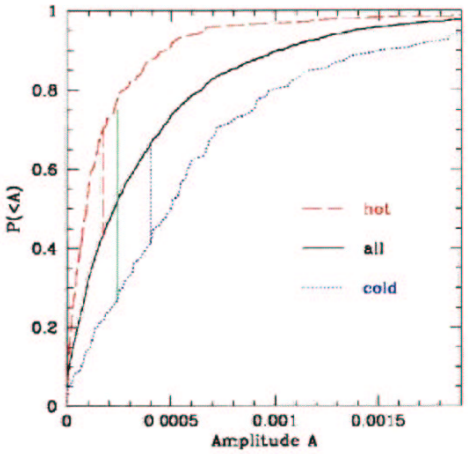

Δ is the maximum difference between the distributions within ∂v=5000km/s window and of all the spectrum

Δ as a function of position for spectrum S1.

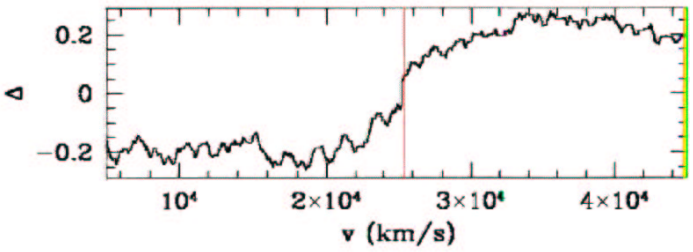

Randomized Spectra

A stretch from QSO 1422+231 spectrum. The randomization is applied to the absorption features marked by the red crosses

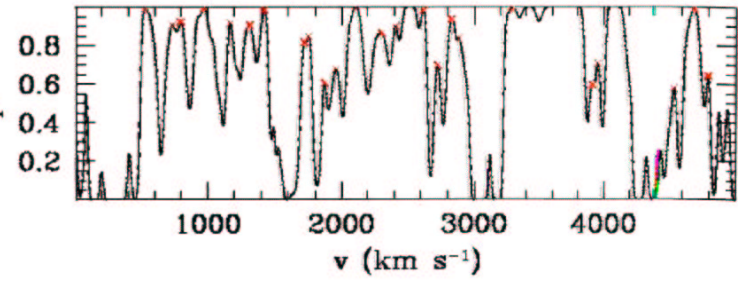

Dotted line: P(Δ) drawn from 200 randomized S1 spectra

Dashed line: P(Δ) of the original S1 but for pairs falling in the same half

Solid line: P(Δ) for pairs that fall in different halves

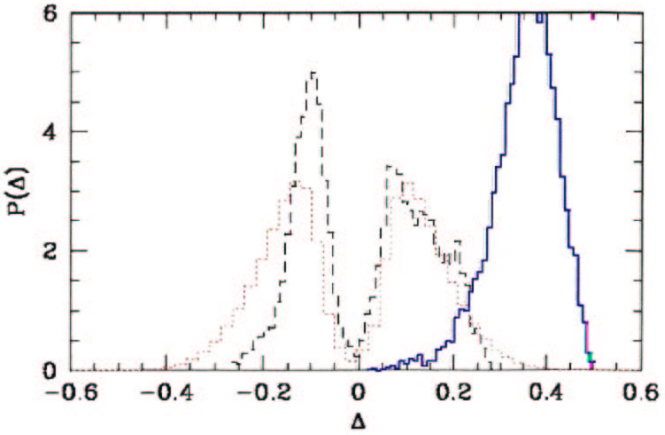

Cluster analysis

$Q(v_1,v_2;\partial v) = \Delta(v_2;\partial v)\,|\Delta(v_1,\partial v;\, v_2,\partial v)|$

Q_l is a the threshold which decide how atypical is Q

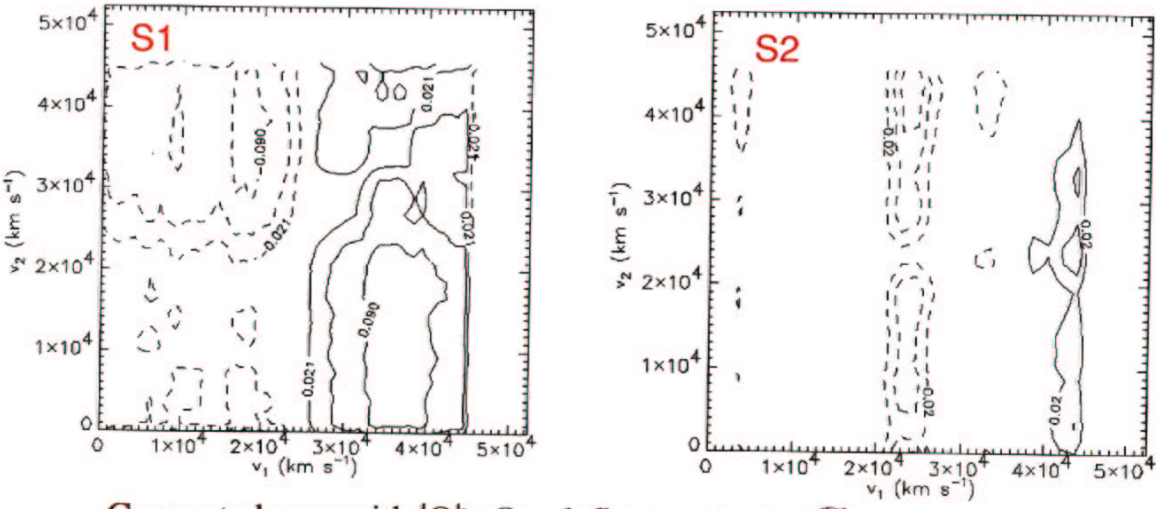

Connected area with $|Q| \geq Q_l$, defines a cluster $\mathbb{C}$

$C(v_1,v_2)$= the integral over $\mathbb{C}$ if $(v_1,v_2) \in \mathbb{C}$

$C(v_1,v_2)$= 0 otherwise.

The final cluster statistic used in the analysis is: $C_P(v_1)=\Sigma_{v_2} C(v_1,v_2)$

We then calculate the probability $P(C_P)$ by performing the same analysis on randomized spectra

$P(C_p)$ for the S1, S2 and S3

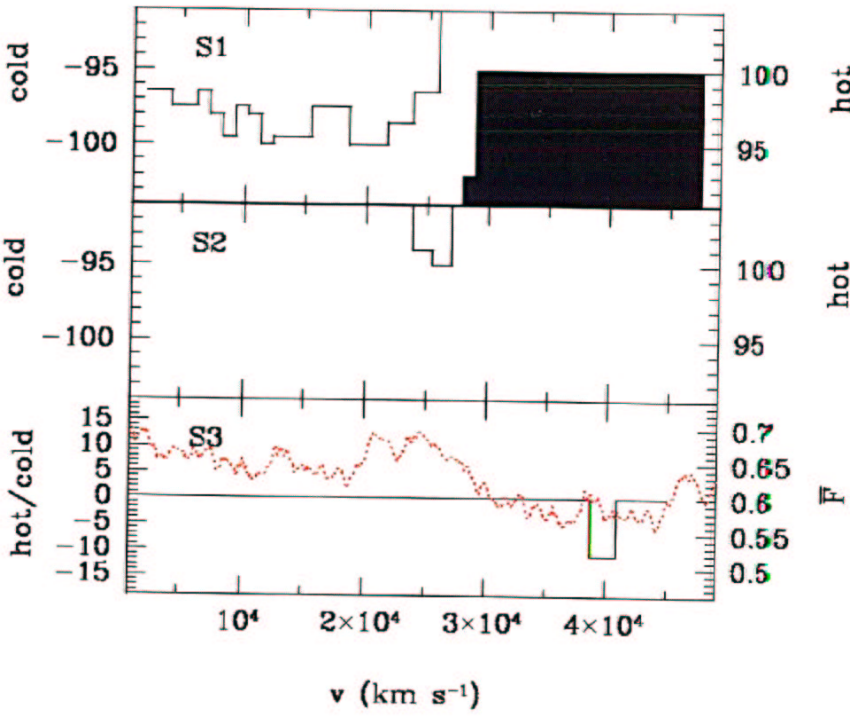

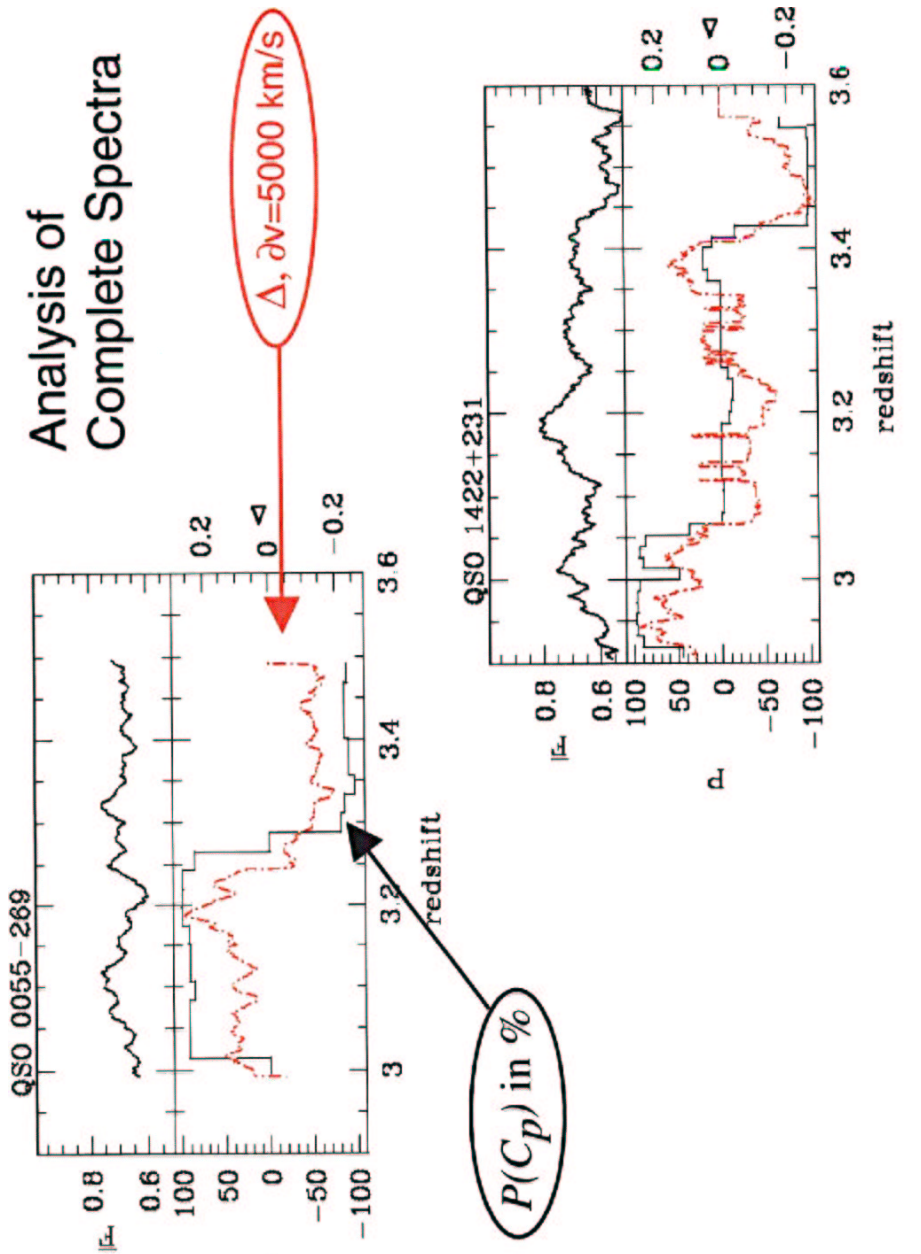
Analysis of
Complete Spectra
QSO 0055−269
QSO 1422+231
Δ, ∂v=5000 km/s
P(C_p) in %
redshift
P
F

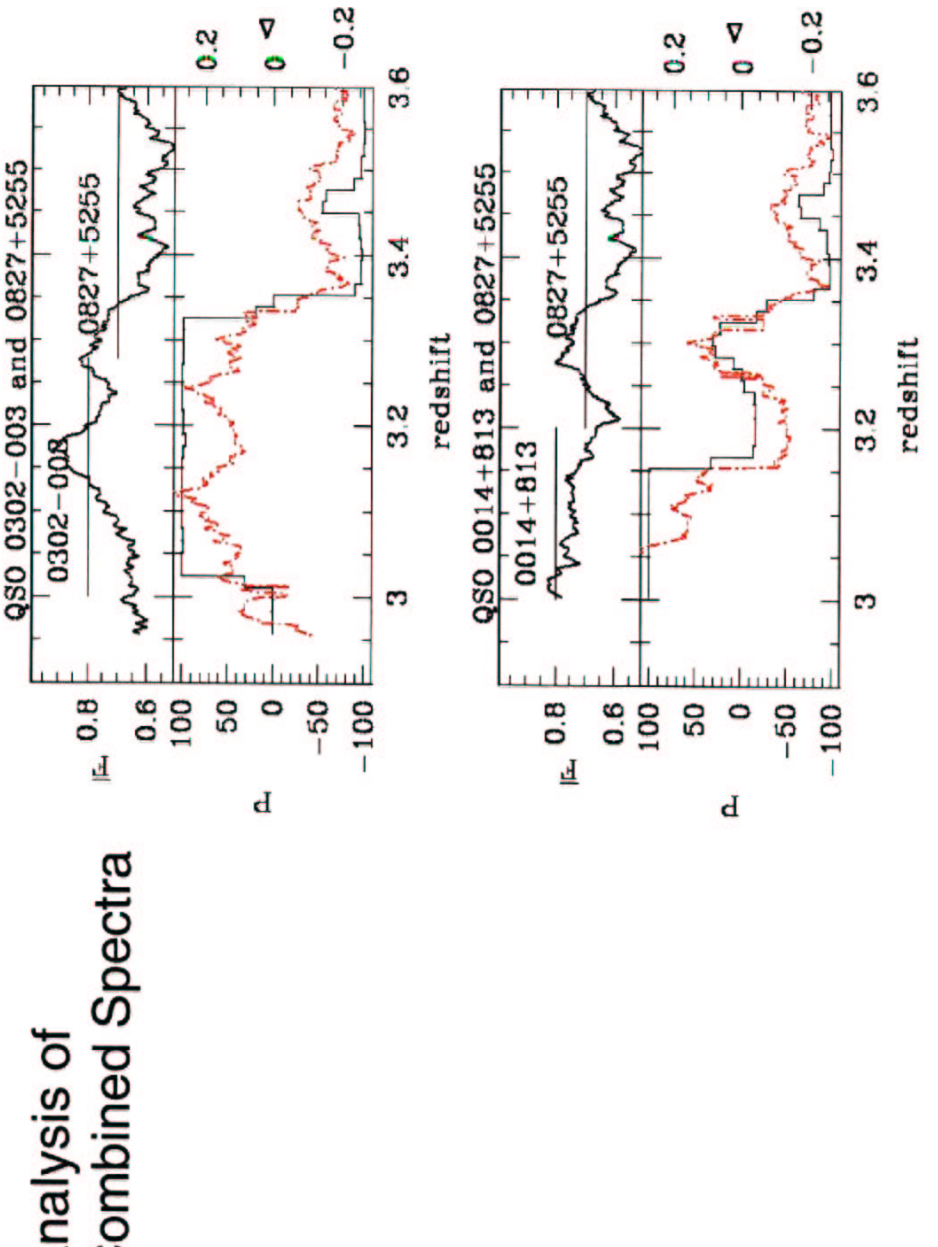
Analysis of
Combined Spectra
QSO 0302−003 and 0827+5255
0302−008
0827+5255
QSO 0014+813 and 0827+5255
0014+813
0827+5255
redshift
P
F

Distribution of Wavelet Amplitude Before and After the Temp. Jump

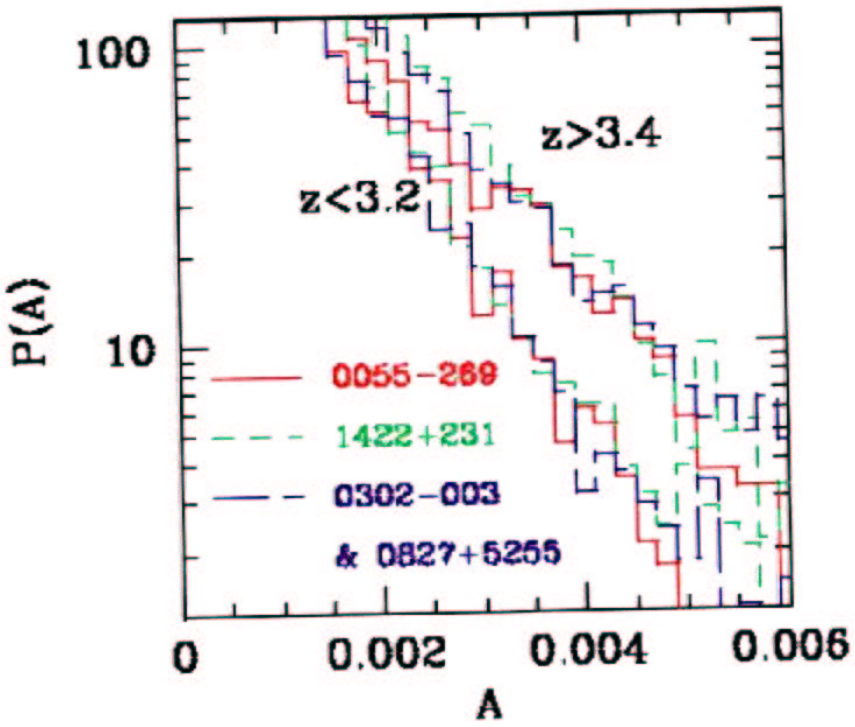

Temperature Calibration

<A> correlates with $T_\delta \equiv T_0 \delta^{\gamma-1}$ at some overdensity δ. Simulations show this strong correlation at δ=1.2. Errors bar come from simulations with single temperature where $T_{1.2}$ varies by 30%.

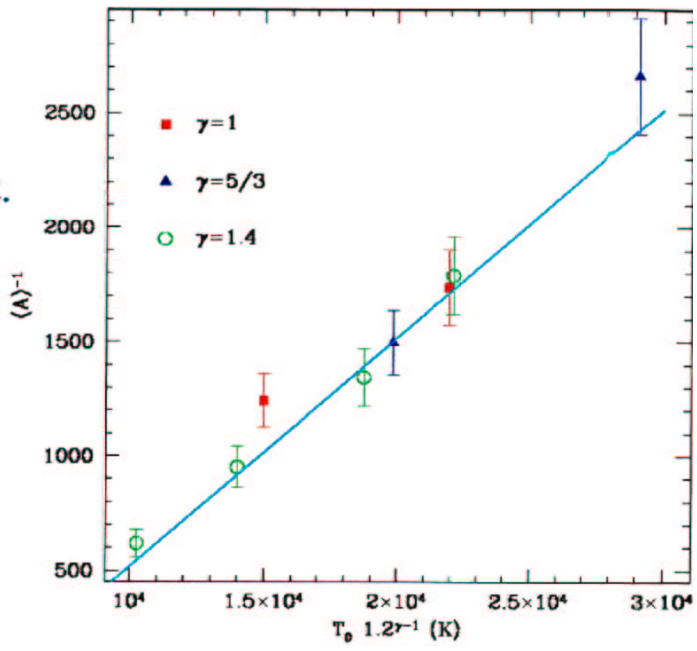

In linear regime this relation holds analytically

Temperature at the mean density, T_0, versus redshift. Open symbols are from Schaye *et al.* 2000.

Filled symbols are from the current work, note that the vertical bars represent error in the determination of T_0 and the horizontal bars denote the redshift extent of the cold/hot region.

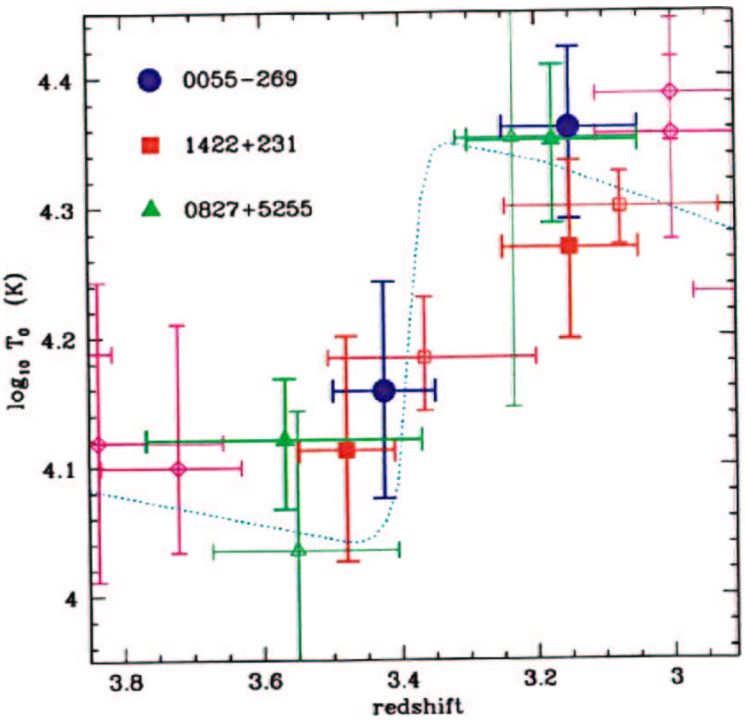

$\Delta T/T_{before} = 60\% \pm 14\%$

SDSS results:

Theuns *et al.* 2002 (astro−ph/0206319)

Bernardi *et al.* 2002 (astro−ph/0206293)

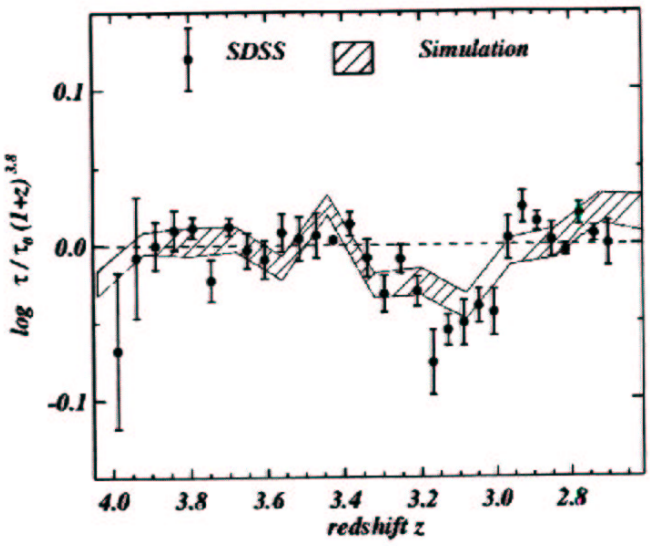

FIG. 3.— Deviation of the effective optical depth from a power-law evolution, $\bar{\tau}_{\rm eff}/(1+z)^{3.8}$, for the SDSS data smoothed on 3000km s^{-1} (symbols with error bars) and a hydrodynamical simulation of a ΛCDM model, in which He II reionization starts at $z = 3.4$ (hashed region). The errors in the SDSS data are determined from bootstrap re-sampling the individual spectra. The hashed region for the simulation delineates the 20 and 80 per centile of bootstrap re-sampled mock samples. The temperature increase associated with He II reionization causes $\bar{\tau}_{\rm eff}$ to drop below the power-law evolution in the simulation. This characterictic dip matches very well the feature detected in the SDSS data.

$$\frac{1}{T_0}\frac{dT_0}{dt}-\frac{1}{\mu}\frac{d\mu}{dt}=-2H_0+\frac{\mu\Delta_\epsilon}{\frac{3}{2}k_BT_0}$$

μ = mean molecular weight

Δ_ε = effective cooling and heating rate.

Recombination, excitation, inverse Compton scattering, collisional ionization & bremsstrahlung

Post HI reionization is $T_0=6\times10^4$K & $\Gamma_{HI}=10^{-13}s^{-1}$

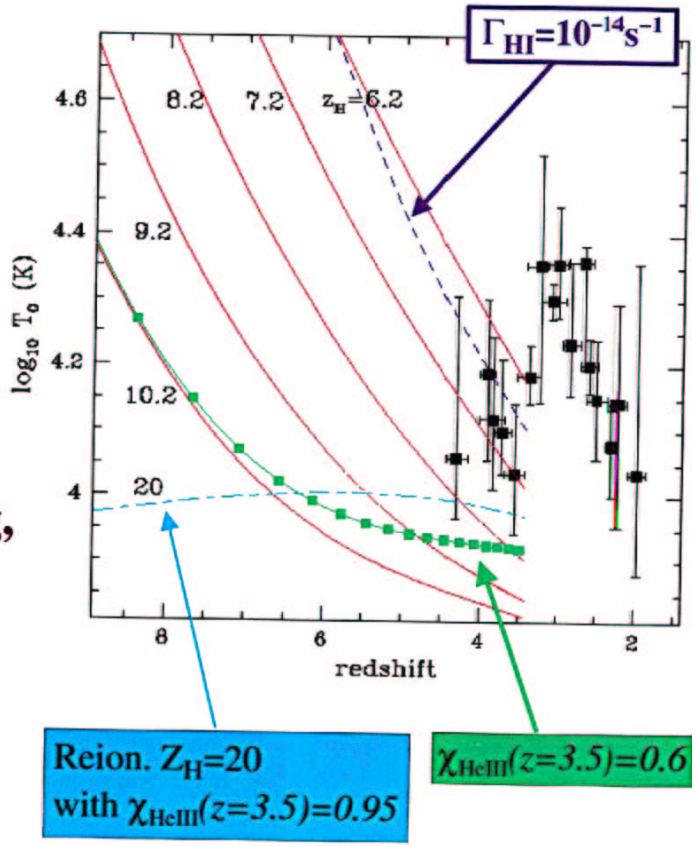

Becker *et al.* 2001 and Djorkovski *et al.* 2001, have observed a sudden increase in the mean flux decrement D_A bluewords of the Ly−α emission of QSO spectra at z~6. This sharp increase might indicate the detection of the onset of H I and He I reionization epoch.